Proceedings of IMECE2010
2010 ASME International Mechanical Engineering Congress and Exposition
November 12-18, 2010, Vancouver, British Columbia, Canada

IMECE2010-40526

OPTIMUM CONFIGURATION OF AN EXPANDING-CONTRACTING-NOZZLE FOR THRUST ENHANCEMENT BY BUBBLE INJECTION

Sowmitra Singh
DYNAFLOW, INC.
www.dynaflow-inc.com
10621-J Iron Bridge Rd, Jessup, MD 20794, USA
Email: sowmitra@dynaflow-inc.com

Jin-Keun Choi
DYNAFLOW, INC.
www.dynaflow-inc.com
10621-J Iron Bridge Rd, Jessup, MD 20794, USA
Email: jkchoi@dynaflow-inc.com

Georges Chahine
DYNAFLOW, INC.
www.dynaflow-inc.com
10621-J Iron Bridge Rd, Jessup, MD 20794, USA
Email: glchahine@dynaflow-inc.com

ABSTRACT

This paper addresses the concept of thrust augmentation through bubble injection into an expanding-contracting nozzle. Two-phase models for bubbly flow in an expanding-contracting nozzle are developed, in parallel with laboratory experiments, and used to ascertain the geometry configuration for the nozzle that would lead to maximum thrust enhancement upon bubble injection.

For preliminary optimization of experimental setup's design, a quasi 1-D approach is used. Averaged flow quantities (such as velocities, pressures, and void fractions) in a cross-section are used for the analysis. The mixture continuity and momentum equations are numerically solved simultaneously, along with equations for bubble dynamics, bubble motion, and an equation for conservation of bubble number. Various geometric parameters such as the exit and inlet areas, the area of the bubble injection section, the presence of a throat and its location, the length of the diffuser section and the length of the contraction section are varied, and their effects on thrust enhancement are studied. Investigation on the effect of the injected void fraction is also carried out. The key objective function of the optimization is the normalized thrust parameter, which is the difference between the thrust with the bubble injection and the thrust before the bubble injection, normalized by the inlet momentum.

An approximate analytical expression for the normalized thrust parameter was also derived starting from the mixture continuity and momentum equations. This analytical expression involved flow variables only at three locations; inlet section, injection section, and outlet section, and the expression is simple enough to produce a quick concept design of the diffuser-nozzle thruster. The numerical and analytical approaches are verified against each other and the limitations of the analytical approach are discussed.

NOMENCLATURE

A : Cross-sectional area
C : Ratio of the exit area to the inlet area
C_b : Sound speed on bubble surface
C_d : Drag coefficient
C_f : Friction coefficient
C_{inj} : Ratio of the exit area to area of the injection section
k : Polytropic gas constant
N : Number of bubbles per unit volume
p : Pressure
p_g : Bubble gas pressure
p_v : Vapor pressure
R : Bubble radius
R_{exit} : Exit radius of the expanding-contracting nozzle
R_{inj} : Radius of injection section of the nozzle
R_{inlet} : Inlet radius of the expanding-contracting nozzle
u_b : Local bubble velocity
u_m : Mixture velocity
α : Void fraction
α_0 : Injected void fraction
β : Volume fraction of liquid $(1-\alpha)$
β_0 : Volume fraction of liquid at injection $(1-\alpha_0)$
γ : Surface tension parameter
μ : Liquid viscosity
ρ_l : Liquid density
ρ_m : Mixture density
ξ_m : Normalized thrust parameter

INTRODUCTION

Recent studies [1,2] have indicated that bubble injection in a waterjet can significantly improve the net thrust and overall propulsion efficiency. The importance of this concept was attributed to the fact that bubble augmented thrust can be achieved even at very high vehicle speeds unlike traditional propulsion devices.

Various analytical, numerical and experimental efforts have been carried out since to formalize the concept of bubble augmented thrust [3,4], and a number of prototypes have been built for experimental verification of this concept [5,6]. In most of these experimental set-ups, the fluid enters a ramjet where it is compressed first by passing through a diffuser (ram effect), then pressurized gas is injected into the fluid via mixing ports, which acts like the energy source of the ramjet. The multiphase mixture is then accelerated through a converging nozzle.

To obtain a first approximation of the mixture flow field inside the air augmented nozzle numerically, one can use classical quasi-one dimensional analyses [7-11]. In such approaches, flow quantities are assumed to be uniform in a direction perpendicular to the axis of the nozzle (i.e. only quantities averaged over a cross-section are used). Early models [12] often neglected the relative motion between the bubbles and the liquid. These effects, however, were later included to account for the inertial effects on bubble dynamics [13]. Furthermore, a more advanced model has been proposed to characterize the bubble dynamics using the Rayleigh-Plesset equation [8-10]. By capturing inertial effects, this model is able to represent transient shock waves in a bubbly mixture. A few recent works [7,14] have used similar models for analyses of bubbly flows in converging diverging nozzles.

Thrust enhancement demonstrations require further modeling and controlled experimentation as we are presently undertaking at DYNAFLOW. One of the primary objectives of our study is to optimize the nozzle geometry for an expanding-contracting nozzle, BAP[1] (Figure 1), in order to obtain good thrust enhancement. In the present paper, two modeling approaches are described. The results from these models serve as good starting guidelines for experimentation.

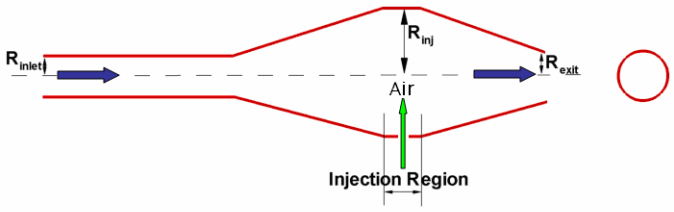

Figure 1. Expanding-contracting Nozzle.

The first approach (1-D BAP) is a one dimensional numerical technique for solving the mixture flow in the nozzle. The second approach (0-D BAP) is purely analytical – derived starting from the mixture continuity and momentum equations in the expanding-contacting nozzle. Even though the second approach has certain limitations, it is very useful in verifying the results from the first approach for simple cases and also for generating quick concept designs.

NUMERICAL PROCEDURE (1-D BAP MIXTURE MODEL)

The unsteady 1-D flow of a bubbly mixture through a nozzle of varying cross-section area, A, can be described by:

$$\begin{aligned} &\frac{\partial \rho_m}{\partial t}+\frac{1}{A}\frac{\partial(\rho_m u_m A)}{\partial x}=0,\\ &\frac{\partial \rho_m u_m}{\partial t}+\frac{1}{A}\frac{\partial(\rho_m u_m A u_m)}{\partial x}+\frac{\partial p}{\partial x}=0, \end{aligned} \tag{1}$$

where ρ_m, u_m and p are the mixture density, velocity and pressure. If we consider the case where the bubbles are injected as a continuous stream, and look for the steady state solution of the cross-section averaged flow quantities, (1) reduces to the following form:

$$\begin{aligned} &\frac{\partial(\rho_m u_m A)}{\partial x}=0,\\ &\frac{1}{A}\frac{\partial(\rho_m u_m A u_m)}{\partial x}+\frac{\partial p}{\partial x}=0. \end{aligned} \tag{2}$$

In this study, the liquid is assumed to be incompressible, i.e. all compressibility effects of the mixture arise from the disperse gas phase alone. By assuming that the density of the injected air/gas is negligible compared to the density of the surrounding liquid, we can express the mixture density in terms of the liquid density, ρ_l and the void fraction, α:

$$\rho_m=\rho_l(1-\alpha). \tag{3}$$

The void fraction, α, is nothing but the volume occupied by the bubbles per unit mixture volume. This can be written using the number of bubbles of radius R_i per unit volume, $N_i(R_i)$:

$$\alpha=\frac{4}{3}\pi\sum_i R_i^3 N_i(R_i). \tag{4}$$

Furthermore, in this paper, we assume that other than at the injection location, no bubbles are created or destroyed. This leads us to the equation of conservation of the number of bubbles:

$$\frac{DN}{Dt}=\frac{\partial N}{\partial t}+\frac{1}{A}\frac{\partial(u_b A N)}{\partial x}=0, \tag{5}$$

[1] BAP: Bubble Augmented Propulsor

where, u_b is the local bubble velocity. This reduces (under the quasi steady assumption) to the following form:

$$\frac{\partial}{\partial x}(u_b AN) = 0 . \tag{6}$$

To describe the dynamics of a local bubble, we assume that the bubble behavior is governed by the modified Keller-Herring equation [15-17]:

$$\begin{aligned}(1-\frac{\dot{R}}{C_b})R\ddot{R}+\frac{3}{2}(1-\frac{\dot{R}}{3C_b})\dot{R} &= \frac{\left(\mathbf{u}_m-\mathbf{u}_b\right)^2}{4} \\ +\frac{1}{\rho_m}(1+\frac{\dot{R}}{C_b}+\frac{R}{C_b}\frac{d}{dt})&\left[p_v+p_g-p-\frac{2\gamma}{R}-4\mu\frac{\dot{R}}{R}\right].\end{aligned} \tag{7}$$

In the above equation, R is the bubble radius, p_g is the bubble gas pressure, C_b is the sound speed on the bubble surface, p_v is the liquid vapor pressure, γ is the surface tension parameter and μ is the dynamic viscosity of the liquid. It is also assumed that the gas inside the bubble follows the polytropic compression law:

$$P_g = p_{g0}\left(\frac{R_0}{R}\right)^{3k}, \tag{8}$$

where, k is the polytropic gas constant, p_{g0} is the initial bubble gas pressure and R_0 is the corresponding initial bubble radius.

The local bubble velocity is obtained by solving the equation for bubble motion [18]:

$$u_b\frac{du_b}{dx}+\frac{3}{\rho_l}\frac{dp}{dx}=\frac{3}{4}(u_m-u_b)\frac{|u_m-u_b|C_d}{R}+3\frac{\dot{R}}{R}(u_m-u_b). \tag{9}$$

In the above equation, C_d is the drag coefficient for a spherical bubble [19]:

$$\begin{aligned}C_d &= \frac{24}{R_{eb}}\left(1+0.197R_{eb}^{0.63}+2.6\times10^{-4}R_{eb}^{1.38}\right); \\ R_{eb} &= \frac{2\rho_m R\,|u_m-u_b|}{\mu}.\end{aligned} \tag{10}$$

Since our approach is quasi-steady, the following space-time transformation is applied for each bubble in order to convert the time derivatives into derivatives along the axial direction:

$$\frac{\partial}{\partial t} = u_b\frac{\partial}{\partial x}. \tag{11}$$

The above set of equations is integrated in space using adaptive embedded explicit Runge-Kutta integration. The difference between the solutions of the 4th and the 5th order accurate schemes is taken as a measure of the integration error and is used to control the forward step size. In addition to the above explicit scheme, an implicit scheme was used for the numerical integration, which made the convergence more robust. The inlet velocity and the exit pressure serve as two convenient boundary conditions.

ANALYTICAL APPROACH (0-D BAP MIXTURE MODEL)

The axisymmetric expanding-contracting nozzle geometry can be defined by the following three cross sectional dimensions (Figure 1):

- Inlet Radius: R_{inlet}
- Injection Radius: R_{inj}
- Exit Radius: R_{exit}

Based on these dimensions, the following contraction area ratios between these sections can be defined:

$$C_{inj} = \left(\frac{R_{exit}}{R_{inj}}\right)^2, \qquad C = \left(\frac{R_{exit}}{R_{inlet}}\right)^2. \tag{12}$$

The velocity and pressure are defined at the three locations as well:

- Velocity and pressure at the inlet: V_{inlet} and p_{inlet} ,
- Velocity and pressure at the injection section: V_{inj} and p_{inj} ,
- Velocity and pressure at the exit: V_{exit} and p_{exit} .

Continuity

When there is no bubble injection, the mass conservation requires:

$$\rho_l R_{inlet}^2 V_{inlet} = \rho_l R_{inj}^2 V_{inj,0} = \rho_l R_{exit}^2 V_{exit,0}, \tag{13}$$

where, the index 0 implies pure liquid. This index is not used at the inlet because we assume that there we always have a pure liquid.

After injection, if we think of the mass flow rate in terms of mixture density and mixture velocity, conservation of mass gives us the following relation:

$$\rho_l R_{inlet}^2 V_{inlet} = R_{inj}^2 \rho_{m,inj} V_{inj,\alpha} = R_{exit}^2 \rho_{m,exit} V_{exit,\alpha}, \tag{14}$$

where, the index α indicates that the fluid is a mixture. Expressing the mixture density at the injection location and at the exit ($\rho_{m,inj}$, $\rho_{m,exit}$) in terms of the liquid density and void fraction (3), we have, after simplification:

$$R_{inlet}^2 V_{inlet} = R_{inj}^2 (1-\alpha_0) V_{inj,\alpha} = R_{exit}^2 (1-\alpha) V_{exit,\alpha}, \quad (15)$$

where, α_0 is the injected void fraction and α is the void fraction at the exit. For convenience, we define:

$$\begin{aligned} \beta_0 &= 1-\alpha_0 \\ \beta &= 1-\alpha \end{aligned}. \quad (16)$$

In our 0-D analysis, we assume no slip between phases i.e. the mixture velocity is same as the liquid velocity at these locations.

Momentum

When there is no injection, using momentum conservation (Bernoulli's equation), we have in the pure liquid:

$$p_{inlet,0} + \frac{\rho_l}{2} V_{inlet}^2 = p_{inj,0} + \frac{\rho_l}{2} V_{inj,0}^2 = p_{exit} + \frac{\rho_l}{2} V_{exit,0}^2. \quad (17)$$

If there is injection, we write the Bernoulli equation separately upstream and downstream of the injection. Applying Bernoulli's equation between the inlet and a point immediately before the injection location (subscript –), we have:

$$p_{inlet,\alpha} + \frac{\rho_l}{2} V_{inlet}^2 = p_{inj^-,\alpha} + \frac{\rho_l}{2} V_{inj^-,\alpha}^2. \quad (18)$$

Applying Bernoulli equation (assuming void faction in the medium is low) between a point immediately after the injection location (subscript +) and the exit, we have:

$$p_{inj^+,\alpha} + \frac{\rho_l}{2}(1-\alpha_o) V_{inj^+,\alpha}^2 = p_{exit} + \frac{\rho_l}{2}(1-\alpha) V_{exit,\alpha}^2, \quad (19)$$

where, the $(1-\alpha_o)$ and $(1-\alpha)$ terms multiplied by ρ_l account for the mixture density.

Applying mass conservation (ignoring air mass) between a point just before the injection (subscript –) and a point just after the injection (subscript +), we have:

$$\rho_l V_{inj-} = \rho_l (1-\alpha_o) V_{inj+} \quad (20)$$

or

$$V_{inj^+} = V_{inj^-} / (1-\alpha_o). \quad (21)$$

Applying momentum balance (ignoring air mass) between a point just before the injection location (subscript –) and a point just after the injection location (subscript +), we have:

$$(p_{inj-} + \rho_l V_{inj-}^2)\pi R_{inj}^2 = (p_{inj+} + \rho_l (1-\alpha_o) V_{inj+}^2)\pi R_{inj}^2. \quad (22)$$

Thus, the pressure jump across the injection location is given as follows:

$$\begin{aligned} \Delta p = p_{inj^-} - p_{inj^+} &= \rho_l V_{inj^-}^2 \frac{\alpha_o}{1-\alpha_o} \\ &= \rho_l V_{inj^+}^2 \alpha_o (1-\alpha_o). \end{aligned} \quad (23)$$

Relationship between Inlet Pressure and Exit Pressure

Using (13) and (15), we have:

$$V_{exit,0} = C^{-1} V_{inlet}, \quad (24)$$

$$V_{exit,\alpha} = \frac{C^{-1}}{(1-\alpha)} V_{inlet}. \quad (25)$$

From continuity between a point after the injection location and the exit (using Eqn.(16)):

$$V_{inj^+,\alpha} = C_{inj} V_{exit,\alpha} (\beta / \beta_0). \quad (26)$$

From continuity between a point before the injection location and the inlet:

$$V_{inj^-,\alpha} = C_{inj} C^{-1} V_{inlet}. \quad (27)$$

Using (18) to (23) in order to relate the inlet pressure and the exit pressure, we have:

$$\begin{aligned} p_{inlet,\alpha} &= p_{inj^-,\alpha} + \frac{\rho_l}{2}\left(V_{inj^-,\alpha}^2 - V_{inlet}^2\right) \\ &= p_{inj^+,\alpha} + \Delta p + \frac{\rho_l}{2}\left(V_{inj^-,\alpha}^2 - V_{inlet}^2\right) \\ &= p_{exit} + \frac{\rho_l}{2}\left(\beta V_{exit,\alpha}^2 - \beta_0 V_{inj^+,\alpha}^2\right) \\ &\quad + \Delta p + \frac{\rho_l}{2}\left(V_{inj^-,\alpha}^2 - V_{inlet}^2\right). \end{aligned} \quad (28)$$

Using (26) and (27), (28) becomes:

$$\begin{aligned} p_{inlet,\alpha} &= p_{exit} + \frac{\rho_l}{2}\left(\beta(\beta_0/\beta)^2 C_{inj}^{-2} - \beta_0\right) V_{inj^+,\alpha}^2 \\ &\quad + \Delta p + \frac{\rho_l}{2}\left(C_{inj}^2 C^{-2} - 1\right) V_{inlet}^2. \end{aligned} \quad (29)$$

Replacing Δp from (23), we have:

$$\begin{aligned} p_{inlet,\alpha} &= p_{exit} + \frac{\rho_l}{2}\left[\beta_0\left(\frac{\beta_0}{\beta} C_{inj}^{-2} - 1\right) V_{inj^+,\alpha}^2\right] + \\ &\quad \frac{\rho_l}{2}\left[\frac{2\alpha_o}{\beta_0} V_{inj^-,\alpha}^2 + \left(C_{inj}^2 C^{-2} - 1\right) V_{inlet}^2\right]. \end{aligned} \quad (30)$$

Expressing V_{inj^+} in terms of V_{inj^-}, by using (21), we get:

$$p_{inlet,\alpha} = p_{exit} + \frac{\rho_l}{2}\left[\frac{\left(\beta_0/\beta C_{inj}^{-2}-1\right)}{\beta_0}V_{inj^-,\alpha}^2 + \frac{2\alpha_o}{\beta_0}V_{inj^-,\alpha}^2 + \left(C_{inj}^2 C^{-2}-1\right)V_{inlet}^2\right]. \quad (31)$$

Expressing V_{inj^-} in terms of V_{inlet}, by using (27), and simplifying, we get:

$$p_{inlet,\alpha} = p_{exit} + \frac{\rho_l}{2}\left[\frac{\left(\beta_0/\beta + \alpha_o C_{inj}^2\right)}{\left(1-\alpha_o\right)C^2} - 1\right]V_{inlet}^2. \quad (32)$$

The above equation is an important approximate relation between the inlet pressure and the exit pressure.

Normalized Thrust Increase

The thrust (without bubble injection) of the expanding-contracting nozzle with circular cross sections is given by:

$$T_R = \pi\left[p_{exit}R_{exit}^2 - p_{inlet,0}R_{inlet}^2 + \rho_l R_{exit}^2 V_{exit,0}^2 - \rho_l R_{inlet}^2 V_{inlet}^2\right]. \quad (33)$$

When there is air injection, the thrust of the expanding-contracting nozzle can be given as follows:

$$T_{R,\alpha} = \pi\left[p_{exit}R_{exit}^2 - p_{inlet,\alpha}R_{inlet}^2 + \rho_l R_{exit}^2\left(1-\alpha\right)V_{exit,\alpha}^2 - \rho_l R_{inlet}^2 V_{inlet}^2\right]. \quad (34)$$

Let us define the normalized thrust gain parameter as follows:

$$\xi_m = \frac{T_{R,\alpha} - T_R}{T_{m-inlet}} = \frac{T_{R,\alpha} - T_R}{\pi\rho_l R_{inlet}^2 V_{inlet}^2}, \quad (35)$$

where, $T_{m-inlet}$ is the inlet momentum rate.

Using expressions (33) and (34) , we have:

$$\xi_m = \frac{-p_{inlet,\alpha} + \rho_l C\left(1-\alpha\right)V_{exit,\alpha}^2 + p_{inlet,0} - \rho_l C V_{exit,0}^2}{\rho_l V_{inlet}^2}. \quad (36)$$

Using (16), and expressing all velocities in terms of the inlet velocity [(24) and (25)], we have:

$$\xi_m = \frac{\left(p_{inlet,0} - p_{inlet,\alpha}\right) + \rho_l C V_{inlet}^2\left[C^{-2}\beta^{-1} - C^{-2}\right]}{\rho_l V_{inlet}^2}. \quad (37)$$

Using equations (17) and(32), we have:

$$p_{inlet,0} - p_{inlet,\alpha} = \frac{\rho_l}{2}\left(C^{-2}-1\right)V_{inlet}^2 - \frac{\rho_l}{2}\left[\frac{\left(\beta_0/\beta + \alpha_o C_{inj}^2\right)}{\left(1-\alpha_o\right)C^2} - 1\right]V_{inlet}^2. \quad (38)$$

Therefore, equation (37) becomes:

$$\xi_m = \frac{1}{2}C^{-2}\left[1 - \left(\frac{\beta_0}{\beta} + \alpha_o C_{inj}^2\right)\beta_o^{-1}\right] + C^{-1}\left(\beta^{-1}-1\right) \quad (39)$$

Relationship between Exit Void Fraction and Injected Void Fraction

An equation relating the injected void fraction, α_0, to the exit void fraction, α, can be derived. Since the injected air obeys the polytropic gas law, we can write:

$$p_{inj^+,\alpha}(\alpha_0)^k = p_{exit}(\alpha)^k. \quad (40)$$

Plugging the above expression in (19), we have:

$$p_{exit}\left[\left(\frac{\alpha}{\alpha_0}\right)^k - 1\right] = \frac{\rho_l}{2}\left[\beta V_{exit,\alpha}^2 - \beta_0 V_{inj^+,\alpha}^2\right]. \quad (41)$$

Using equation (26) in the above expression to replace $V_{inj^+,\alpha}$, we have:

$$p_{exit}\left[\left(\frac{\alpha}{\alpha_0}\right)^k - 1\right] = \frac{\rho_l}{2}V_{exit,\alpha}^2\beta\left[1 - \beta_0^{-1}\beta C_{inj}^2\right]. \quad (42)$$

Using expression (25) in the above equation, we have:

$$p_{exit}\left[\left(\frac{\alpha}{\alpha_0}\right)^k - 1\right] = \frac{\rho_l}{2}V_{inlet}^2 C^{-2}\beta^{-1}\left[1 - \frac{\beta}{\beta_0}C_{inj}^2\right]. \quad (43)$$

Therefore,

$$\alpha = \alpha_0\left[1 + \frac{\rho_l}{2p_{exit}}V_{inlet}^2 C^{-2}\beta^{-1}\left(1 - \frac{\beta}{\beta_0}C_{inj}^2\right)\right]^{1/k}. \quad (44)$$

Given α_0, the above equation is solved iteratively to obtain α and hence β.

RESULTS AND DISCUSSION

Validation of 1-D BAP

Independent studies [3] were conducted at DYNAFLOW using 1-D BAP for a particular expanding-contracting nozzle configuration and the results were verified against results from our Discrete Bubble Model (DBM) – 3DYNAFS_DSM©, coupled with FLUENT. Figure 2 indicates that the total thrust predicted by the 1-D Quasi steady (1-D BAP) model compares well with results from DBM coupled with Fluent.

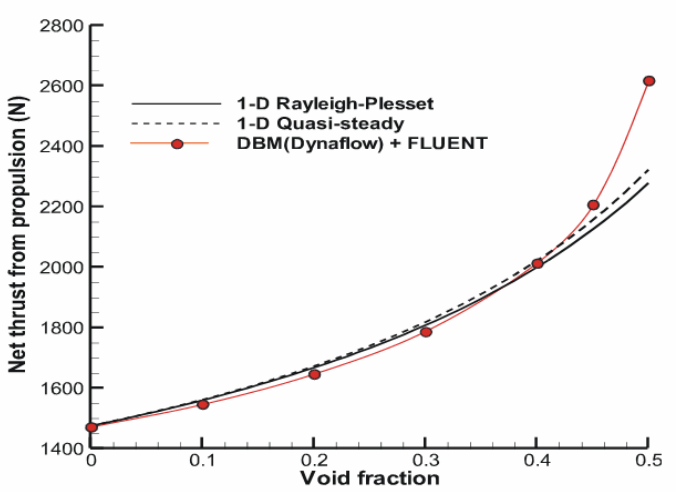

Figure 2. Comparison of the total thrust obtained using different approaches [3].

Dependence of Normalized Thrust Parameter on Contraction Area Ratio *C*

The analytical expression for ξ_m (obtained using 0-D BAP) was compared against results from the 1-D BAP code. Figure 3 shows the length dimensions of the expanding-contracting nozzle under study. The 1-D BAP runs were carried out for different values of *C* (ratio of the exit area to the inlet area defined in (12)). The runs were carried out using two inlet velocities of 2.4 m/s and 3.57 m/s, an exit pressure of 101,325 Pa and a R_{inj} of 9.35 cm.

Figure 4 shows the variations of the normalized thrust parameter (ξ_m) with variation of *C* (varying R_{exit}) for an inlet velocity of 2.4 m/s. The curves have an optimum close to *C=1*. Also, as expected, the normalized thrust parameter is higher for higher injected void fraction. It must be noted that the analytical expression compares better with the numerical results when the injected void fraction is small. Figure 5 shows a similar set of results for an inlet velocity of 3.57 m/s. The 1-D BAP curves for these two inlet velocities are almost identical. The analytical results, on the other hand, are slightly different for the two cases. For a higher inlet velocity, the analytical approach predicts much higher thrust gain. This is because the computed exit void fraction [from equation(44)] is significantly higher than the injected void fraction when the inlet velocity is large. Even though this effect is expected in reality, 1-D BAP results suggest that the 0-D model over-predicts the thrust gain for larger inlet velocities. As mentioned earlier 1-D BAP shows similar trends, i.e. the thrust gain increases when the inlet velocity increases (Figure 6). However, the inlet velocity must be large (10 m/s for the case shown in Figure 6) to see significant improvement in thrust gain.

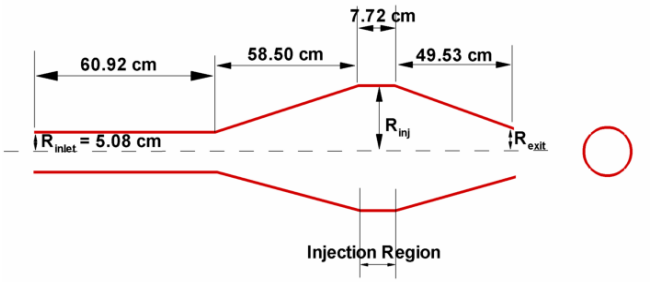

Figure 3. Dimensions of the expanding-contracting nozzle.

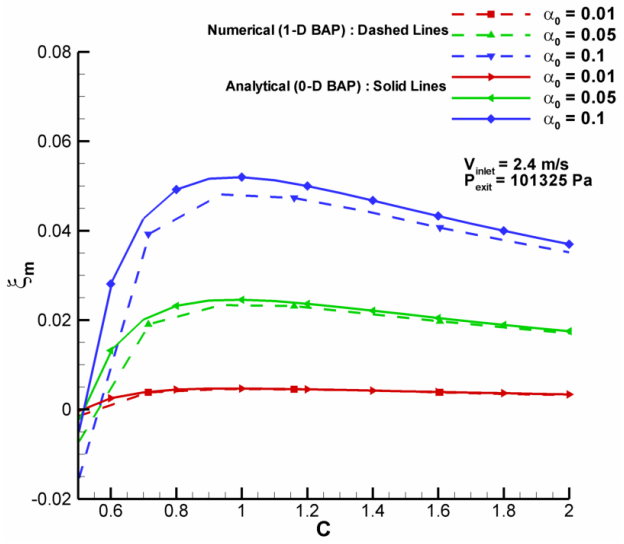

Figure 4. Normalized thrust parameter versus C (V_{inlet} = 2.4 m/s). Analytical expression for ξ_m is compared against results from the 1-D BAP code.

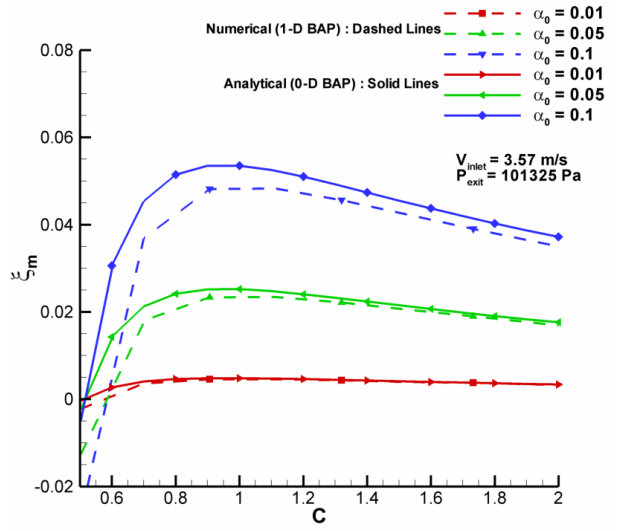

Figure 5. Normalized thrust parameter versus C (V_{inlet} =3.57 m/s). Analytical expression for ξ_m is compared against results from the 1-D BAP code.

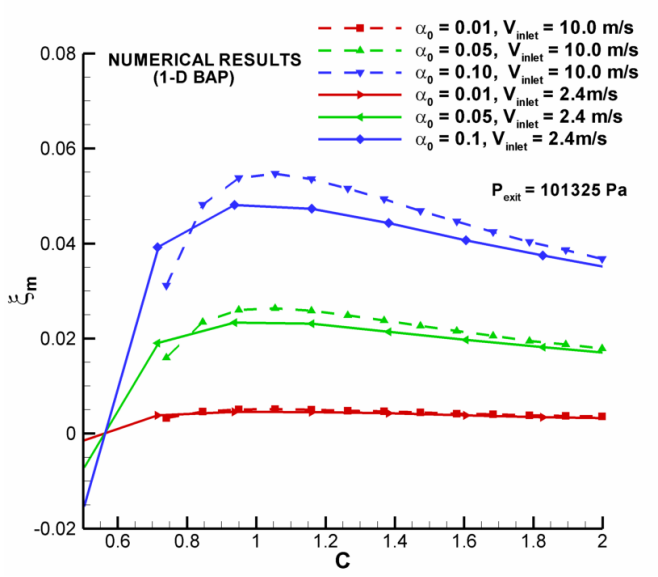

Figure 6. Effect of increasing the inlet velocity on Normalized thrust parameter: 1-D BAP.

In addition, one can observe from equation (39) that for C=1, $\xi_m \approx \alpha_0/(1-\alpha_0)\times\left[(1-C_{inj}^2)/2\right]$ (assuming $\alpha=\alpha_0$). Figure 7 shows the variation of ξ_m with variation of the injected void fraction α_0 as obtained from the two approaches (for C=1). The results reaffirm the fact that increasing the injection void fraction increases thrust gain.

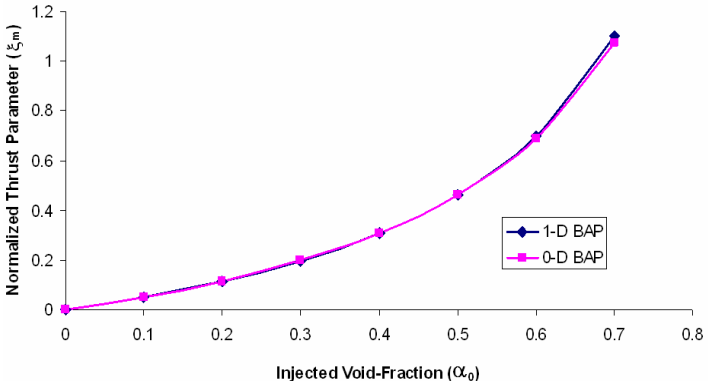

Figure 7. Normalized thrust parameter versus injected void fraction:C=1.

Dependence of Normalized Thrust Parameter on Contraction Area Ratio C_{inj}

Physical intuition suggests that increasing the ratio of the injection area to the exit area would increase the normalized thrust gain. This is because, increasing the injection area would imply that the bubbles are injected at a higher flow pressure and their expansion at the exit (lower pressure) would prominently cause the liquid at the exit to flow out with higher velocity, contributing to higher thrust.

Figure 8 and Figure 9 capture the variation of ξ_m with the variation of $1/C_{inj}$ for two different values of α_0. In these runs, C is fixed at 1.1 (close to optimum). It appears that increasing the area of the injection region does not have significant effect on the normalized thrust parameter beyond a certain limit. For instance, when α_0 =0.05, ξ_m for $1/C_{inj}$=6 is approximately 95% of the value of ξ_m for $1/C_{inj}$=12.

Again, the 0-D BAP captures the trend better when the injected void fraction is small.

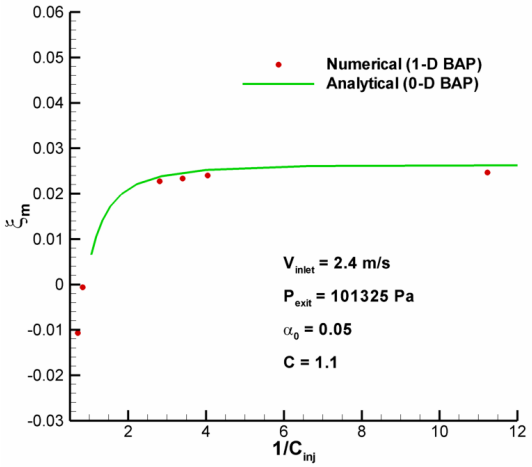

Figure 8. Normalized thrust parameter versus 1/Cinj - α_0 =0.05, C=1.1.

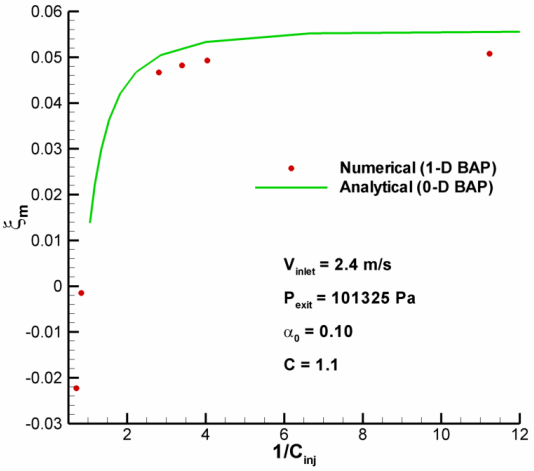

Figure 9. Normalized thrust parameter versus 1/Cinj - α_0 =0.10, C=1.1.

Presence of a Throat

After establishing that the normalized thrust parameter is optimum for C=1, we studied the effect of the presence of a throat just before the exit of the expanding-contracting nozzle. Starting with a basic configuration, Figure 10a, two modifications are applied. The first modification involves reducing the length of the contraction section, Figure 10b, and the second modification involves extending the length of the contraction section, Figure 10c, in order to incorporate a throat. It must be noted that both these modifications ensure that C=1. Within the second modification, different configurations were tried. These configurations, essentially, determine the size of the throat (Figure 11). Configuration 1 has no throat [dashed line in Figure 10 (c)] while Configuration 10 has a very narrow throat.

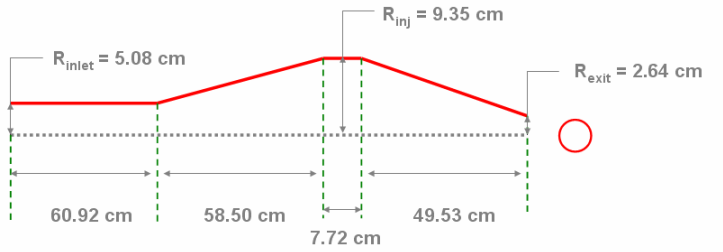

(a) Basic Configuration

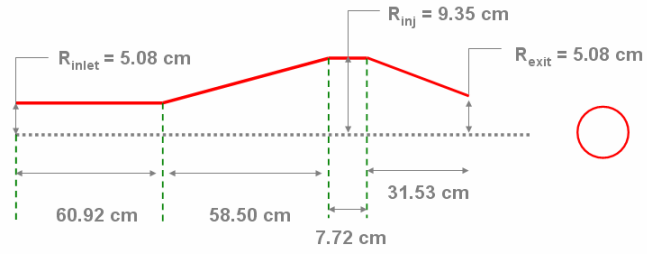

(b) Cut Exit

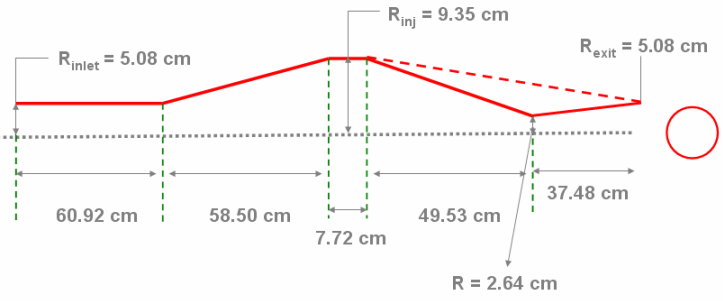

(c) Extended Exit

Figure 10. Geometry of the expanding-contracting nozzle.

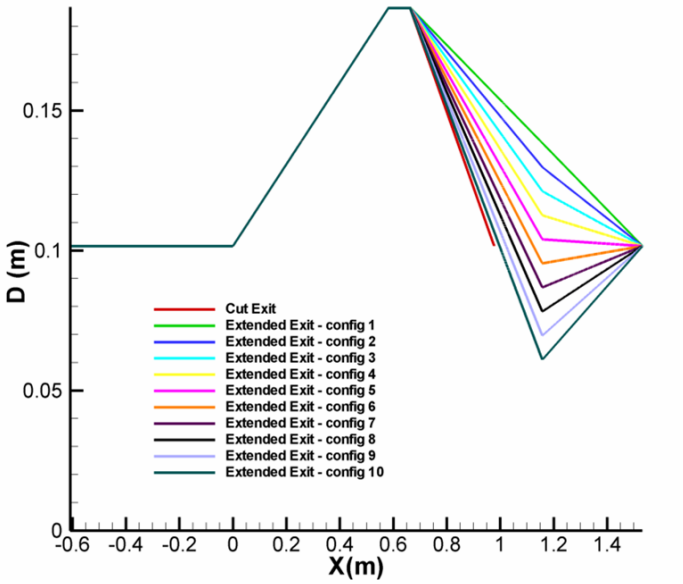

Figure 11. Different configurations (expanding-contracting nozzle) studied.

Figure 12 shows the variation of the normalized thrust parameter, ξ_m, with variation of the injected void fraction, and Figure 13 shows the variation of the total thrust versus variation of α_0 for an inlet velocity of 2.4 m/s.

Since the 0-D BAP analytical approach only involves the area ratios C and C_{inj} and does not include the geometry variation occurring in-between, it cannot capture the trends when a throat is introduced before the exit. The results from 1-D BAP for cut-exit match the 0-D BAP results quite well (Figure 12).

From the 1-D BAP results, it appears that introducing a throat is not beneficial in increasing thrust gain. This is somewhat contrary to physical intuition. One would expect the presence of a throat to accelerate the liquid (due to bubble expansion) and consequently improve thrust gain. In order to confirm the trend for other flow conditions, a simulation with a higher inlet velocity was performed. It was thought that having higher flow velocity would lead to a higher void fraction in the throat region and would consequently increase thrust gain. Figure 14 shows the variation of the normalized thrust parameter, ξ_m, with the variation of the injected void fraction for selected configurations at the inlet velocity of 10m/s. Even in this case, presence of a throat did not help in achieving higher thrust gain.

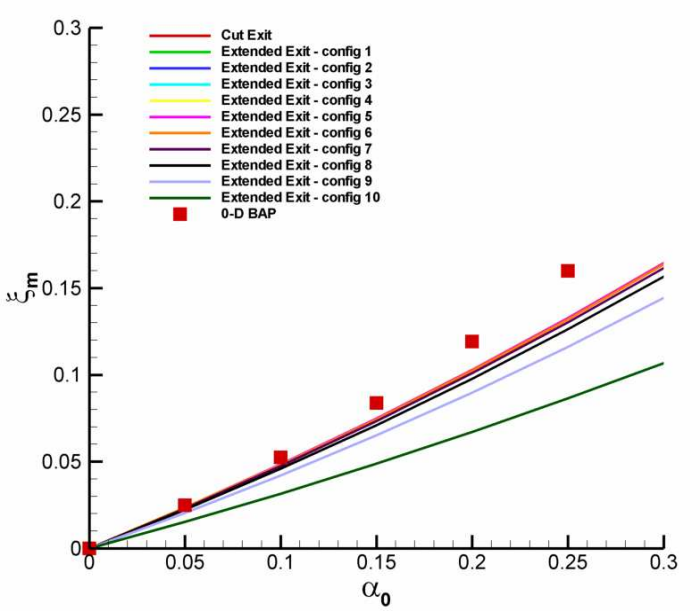

Figure 12. Normalized thrust parameter versus injected void fraction (different configurations, C=1, V_{inlet} =2.4 m/s).

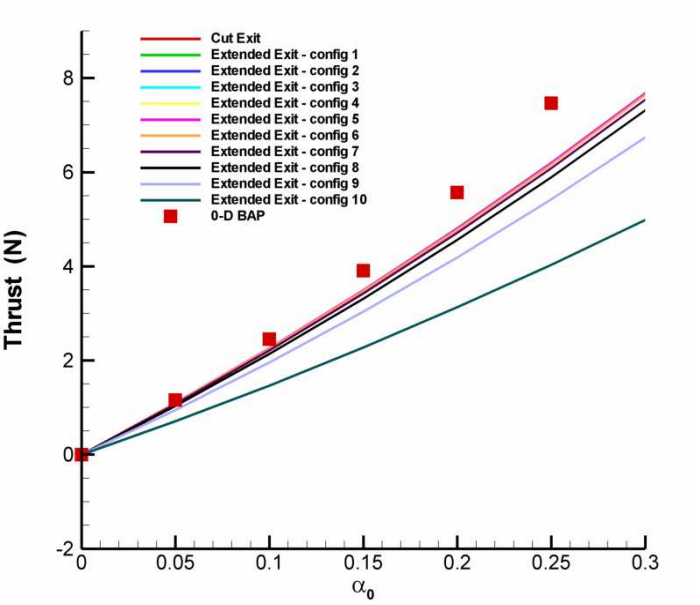

Figure 13. Total thrust versus injected void fraction (different configurations, C=1, V_{inlet} =2.4 m/s).

CONCLUSION

One of the primary objectives of this study was to optimize the geometry of an expanding-contracting nozzle in order to obtain high thrust enhancement. To achieve this, two modeling approaches were followed. The first approach (1-D BAP) used a quasi one dimensional numerical technique for solving the mixture flow in the nozzle. The second approach (0-D BAP) involved analytical derivation of the normalized thrust parameter.

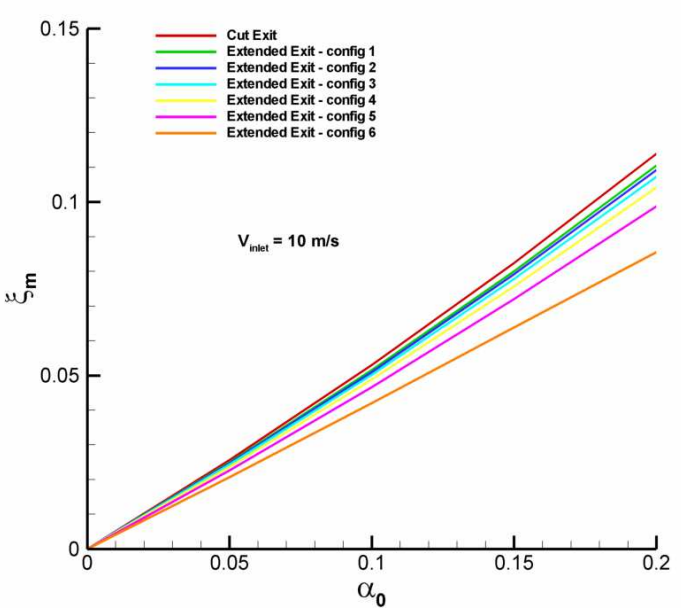

Figure 14. Normalized thrust parameter versus injected void fraction (different configurations, C=1, V_{inlet} =10 m/s).

The analytical approach is very useful in providing physical understandings of the bubbly flow phenomenon in the nozzle, verifying the results of the first approach, and generating quick concept designs. On the other hand, the first approach, with the use of numerical solutions, can predict the nozzle performance more accurately with more detailed considerations including the followings:

1) The approach accounts for the dynamics of individual bubbles in the mixture.
2) The approach allows slip between the bubble and the mixture flow around.
3) The approach includes the geometric variation along the nozzle including multiple contractions. Hence, it can capture the effect of a throat if exists.

An even further complete approach involving 3D computation coupling an Eulerian viscous computation with a Lagrangian discrete bubble description is presented elsewhere [3,4]. For simple configurations, it was found that the maximum normalized thrust gain occurs when the exit area is equal to the inlet area. Additionally, the thrust gain is higher for higher injected void fraction. It was also found that increasing the area of the injection region (relative to the exit) increases the normalized thrust gain to a certain extent.

Moreover, the 1-D BAP simulations indicated that the presence of a throat under the conditions we have studied reduces thrust gain. This conclusion should be reexamined with further analysis and experiments since the 1-D BAP code does not capture the complex flow physics (e.g. separation, compressibility of the mixture, non-uniformity in radial direction etc.) that would prevail in the presence of a throat.

ACKNOWLEDGMENTS

This work was conducted at DYNAFLOW as a part of support by the Office of Naval Research under contract N00014-09-C-0676, monitored by Dr. Ki-Han Kim. This support is acknowledged with gratitude.

REFERENCES

1. Albagli, D. and Gany, A. "High Speed Bubbly Nozzle Flow with Heat, Mass, and Momentum Interactions", *International Journal of Heat and Mass Transfer*, 46, 1993-2003, 2003.
2. Mor, M. and Gany, A. "Analysis of Two-Phase Homogeneous Bubbly Flows Including Friction and Mass Addition", *Journal of Fluids Engineering Transaction of the ASME*, **126**, 102-109, 2004.
3. Chahine, G. L., Hsiao, C.-T., Choi, J.-K. and Wu, X. "Bubble Augmented Waterjet Propulsion: Two-Phase Model Development and Experimental Validation", *Proc. 27th Symposium on Naval Hydrodynamics, Seoul, Korea*, October 5-10, 2008.
4. Wu, X., Choi, J.-K., Hsiao, C.-T., and Chahine, G.L., "Bubble Augmented Waterjet Propulsion: Numerical and Experimental Studies", *Proc. 28th Symposium on Naval Hydrodynamics*, Pasadena, California, September 2010.
5. Mottard, E.J. and Shoemaker, C.J. "Preliminary Investigation of an Underwater Ramjet Powered by Compressed Air", NASA Technical Note D-991, 1961.
6. Schell Jr., et al., "The Hydro-Pneumatic Ram-Jet", US Patent 3,171,379, 1965.
7. Wang, Y.-C. and Brennen, C.E., "One-Dimensional Bubbly Cavitating Flows through a Converging-Diverging Nozzle", *Journal of Fluids Engineering*, Vol. 120, pp. 166-170, 1998.
8. Van Wijngaarden, L., "Linear and Non-linear Dispersion of Pressure Pulses in Liquid Bubble Mixtures", *Proc. 6th Symposium on Naval Hydrodynamics*, ONR, 1966.
9. Van Wijngaarden, L., "On the Equations of Motion for Mixtures of Liquid and Gas Bubbles", *Journal of Fluid Mechanics*, Vol. 33, pp. 465-474, 1968.
10. Van Wijngaarden, L., "One-Dimensional Flow of Liquids Containing Small Gas Bubbles", *Annual Review of Fluid Mechanics*, Vol. 4, pp. 369-396, 1972.
11. Noordzij, L. and van Wijngaarden, L., "Relaxation Effects Caused by Relative Motion on Shock Waves in Gas-Bubble/Liquid Mixtures", *Journal of Fluid Mechanics*, Vol. 66, pp. 15-143, 1974.
12. Tangren, R.F., Dodge, C.H., and Seifert, H.S., "Compressibility Effects in Two-Phase Flow", *Journal of Applied Physics*, Vol. 20 No. 7, pp. 637-645, 1949.
13. Ishii, R., Umeda, Y., Murata, S., and Shishido, N., "Bubbly Flows through a Converging-Diverging Nozzle", *Physics of Fluids*, Vol. 5, pp. 1630-1643, 1993.
14. Preston, A., Colonius, T., and Brennen, C.E., "A Numerical Investigation of Unsteady Bubbly Cavitating Nozzle Flows", *Proc. of the ASME Fluid Engineering Division Summer Meeting*, Boston, 2000.
15. Gilmore, F. R., "The Growth and Collapse of a Spherical Bubble in a Viscous Compressible Liquid", California Institute of Technology, Div. Rep. 26-4, Pasadena, CA, 1952.
16. Knapp, R.T., Daily, J.W., Hammit, F.G., *Cavitation*, ed. Hill, M., New York, 1970.
17. Vokurka, K., "Comparison of Rayleigh's, Herring's, and Gilmore's Models of Gas Bubbles", *Acustica*, Vol. 59, No. 3, pp. 214-219, 1986.
18. Johnson, V.E. and Hsieh, T., "The Influence of the Trajectories of Gas Nuclei on Cavitation Inception", *Proc. Sixth Symposium on Naval Hydrodynamics*, pp. 163-179, 1966.
19. Haberman, W.L. and Morton, R.K., "An Experimental Investigation of the Drag and Shape of Air Bubbles Rising in Various Liquids", Report802, DTMB, 1953.